# Lycorine Inhibits Angiogenesis by Docking to PDGFRα

**Fei Lv**
Shengjing Hospital of China Medical University
**XiaoQi Li**
Shenyang Tenth People's Hospital
**LiYing Hao**
China Medical University
**Ying Wang** ( wang_ying@sj-hospital.org )
Shengjing Hospital of China Medical University

**Research Article**

**Keywords:** Angiogenesis Inhibitors, Lycorine, Molecular Docking Simulation, Receptor, Platelet-Derived Growth Factor alpha

**Posted Date:** February 17th, 2022

**DOI:** https://doi.org/10.21203/rs.3.rs-1327411/v1

# Abstract

Lyc (Lycorine) is a natural alkaloid derived from medicinal plants of the Amaryllidaceae family. Lyc has been reported to inhibit recurrence and metastasis of different kinds of tumors. However, the Lyc's effect of angiogenesis and its specific mechanism is still not clear. This study was designed to test the anti-angiogenesis effect of Lyc and explore possible mechanisms. We performed cell experiments to confirm Lyc's inhibitory effect on angiogenesis and employed sunitinib as a positive control. Meanwhile, the synergistic effect of Lyc and sunitinib was also explored. Next, we conducted bioinformatics to predict the potential targets of Lyc and verified them by western blott and immunofluorescence. Molecular docking, kinase activity assays, Biacore assays and cellular thermal shift assays (CETSAs) were applied to elucidate the mechanism by which Lyc inhibited target activity. Lyc inhibited angiogenesis in human umbilical vein endothelial cells (HUVECs). Employing bioinformatics, we found that Lyc's target was PDGFRα and that Lyc attenuated PDGFRα phosphorylation. We also found that Lyc inhibited PDGFRα activation by docking to it to restrain its activity. In addition, Lyc significantly inhibited PDGF-AA-induced angiogenesis. This study provides new insights into the molecular functions of Lyc and indicates its potential as a therapeutic agent for tumor angiogenesis.


# Introduction

Malignant tumors are the main cause of death and important obstacles to improving life expectancy worldwide [1]

Angiogenesis is one of the hallmarks of tumors [2], and tumor blood vessels provide oxygen and nutrition for tumors, enabling rapid growth and providing a path for distal metastasis [3, 4]. When tumor growth is greater than 2 $mm^3$, the vasculature on the tumor surface is disordered. This is conducive to the exogenous growth of tumors and prevents drugs from entering the tumor body resulting in reduced drug uptake, which is the theoretical basis for the treatment of tumors with anti-angiogenic drugs [5]. Although some anti-angiogenic drugs have been developed for cancer treatment, their effect is limited. Taking liver cancer as an example, the estimated rate of survival after 12 months of treatment with anti-angiogenic drugs was only approximately 50% [6]. In addition, adverse events, such as hypertension and rash, which are caused by blocking vascular growth, greatly limit the application of these drugs [7, 8]. Therefore, it is necessary to find new anti-angiogenic drugs to treat tumors.

In recent years, natural compounds have been proven to be effective in the treatment of tumors, including in anti-angiogenesis[9-11]. Lyc (Lycorine) is a natural alkaloid derived from medicinal plants of the Amaryllidaceae family[12] that have a series of bioactivities, including anti-inflammation[13], anti-viral[14], anti-fungal[15], and especially antitumor activities[16, 17]. For example, Hu et al.[18] found that Lyc directly interacted with EGFR and inhibited EGFR activation to treat glioma. Lyc can also inhibit other tumor types, including hepatocellular carcinoma[19], lung cancer[20] and osteosarcoma[21], without remarkable toxicity[22, 23]. Lyc can also inhibit vasculogenic mimicry by reducing VE-cadherin gene expression in

melanoma[24] and ovarian cancer[25]. However, Lyc's effect on angiogenesis and its specific mechanism are still not clear.

Bioinformatics is a research method used in the identification of new drug targets based on a network perspective[26]. In pharmacological research of natural compounds, bioinformatics can integrate complex components, targets, and diseases. Here, PharmMapper and other databases were used to study Lyc's targets for the first time, revealing PDGFRα as the main target. A good spatial and energy match was found between Lyc and PDGFRα using molecular docking, which was further confirmed by a series of experiments.

In this study, we explored the anti-angiogenic roles of Lyc in vitro and in vivo, employing sunitinib as a positive control, and then the Lyc targets were predicted by the PharmMapper database. Lyc inhibited PDGFRα activities by docking to it directly. This protocol can be considered an effective method for exploring completely new applications of natural products with exact structural formulas. This study improved the understanding of Lyc's molecular biological function and indicated that Lyc may be a promising anti-angiogenic therapy.

# Materials And Methods

### Cell lines and Reagents

Human Umbilical Vein Endothelial Cells (HUVECs) were purchased from Cell Bank of Representative Culture Preservation Committee of Chinese Academy of Sciences (Shanghai, China). HUVECs were cultured in HUV-EC-C medium and kept in an incubator at 37°C with 5% $CO_2$.

Lyc was purchased from MedChemExpress (HY-N0288) and prepared as described before[27]. Sunitinib and PDGF-AA were also purched from MedChemExpress (HY-10255A; HY-P70598).

### MTT

Cell viability was examined using the 3-(4,5-dimethylthiazol-2-yl)-2,5-diphenyltetrazolium bromide (MTT) assay. Cells (3000 cells/well) were seeded in a 96-well plate overnight and then exposed to different concentrations of Lyc (and/or sunitinib) and incubated for 24 and 48 h. A total of 20 μL of MTT solution (5 mg/mL, Sigma, M5655) were added to each well and the cells were incubated for another 4 h at 37°C. The supernatant was then removed and 200 μL of DMSO were added to each well to dissolve the precipitate. Absorbance was measured using a spectrophotometer (BIOBASE, EL10A) at 490 nm.

### Colony Formation

Cells were seeded in six-well plates at a density of 1000 cells/well. On the next day, cells were treated with Lyc and/or sunitinib. Ten days after the treatment, cells were fixed with methanol for 15 min and then staixned with 0.1% crystal violet. Finally, stained cell colonies were photographed with a digital camera and analyzed using ImageJ (National Institutes of Health (NIH), Bethesda, USA).

### Flow Cytometry

Cells cultured in a Petri dish and treated with Lyc and/or sunitinib for a range of time points were collected and incubated with 5 μL of Annexin V and 10 μL of PI for 15 min in the dark. The samples were then evaluated using flow cytometry and the data were analyzed using FlowJo (TreeStar, USA).

### Transwell Assay

For the migration assay, 200 μL of HUV-EC-C medium containing cells (2.0 x $10^4$ cells/chamber) and different concentrations of Lyc (and/or sunitinib) were seeded in an upper Transwell chamber (Corning 3422, USA). HUV-EC-C medium containing 25 ng/mL PDGF-AA was added to the lower chamber. Non-migrated cells from the upper membrane were removed after incubation for 24 h at 37°C. The migrated cells were stained with 0.1% crystal violet and photographed under a light microscope at x 200. Migrated cells were analyzed quantitatively using ImageJ.

### Wound Healing

Cells (2 x $10^5$ cells/well) were seeded in six-well plates. As the cells became sub-confluent, a straight cell-free wound was scratched with a 10 μL pipette tip. Cells were then washed twice with PBS and incubated in serum-free medium containing different concentration of Lyc and/or sunitinib. Cell scratches were observed and measured at different time points. Cell migration distances were analyzed quantitatively using ImageJ.

### Tube Formation

HUVECs were plated at a density of 1 x $10^4$ cells/well in 96-well flat-bottomed plates after Matrigel (BD Biosciences, USA) pre-coating at 37°C for 30 min. Thereafter, HUVECs were treated with different concentrations of Lyc and/or sunitinib for 4 h. After exposure, HUVECs tubes and branches were photographed under a light microscope at x 200. The formed branches were analyzed quantitatively using ImageJ.

### Chick Chorioallantoic Membrane (CAM) Model

Five fresh 10-day-old fertile eggs were cleaned with alcohol and then incubated at 37°C and 60-80% humidity in an egg incubator. The shell was cut to create a small window (20 x 20 $mm^2$) and the shell membrane was removed with sterile forceps to expose the chorioallantoic membrane. A small rubber ring was placed on the chorioallantoic membrane and different concentrations of Lyc and/or sunitinib were added into the ring and incubated. At baseline and 8, 16 h later, the ring area was photographed by a scanner and the images were analyzed using Image-Pro Plus 6.0 (Epix, USA).

### Bioinformatics Prediction

Lyc's structural formula was drawn using Chemdraw (ChemBioOffice, CambridgeSoft, USA) and uploaded to PharmMapper[28] (http://59.78.96.61/pharmmapper/) to obtain possible Lyc targets. The target names were then corrected to the official symbol using UniProt (https://www.uniprot.org/). Gene ontology (GO) functional annotation[29] and Kyoto Encyclopedia of Genes and Genomes (KEGG) pathway analysis[30, 31] of the Lyc-related targets were performed using WebGestalt (http://www.webgestalt.org/)[32]. Biological processes, molecular functions, and cellular components of the target were visualized using the ggplot2 package in R. Angiogenesis-related targets were obtained using GeneCards (www.genecards.org/) and intersected to the predicted targets in order to get possible Lyc targets for angiogenesis-inhibiting. Finally, target names were submitted to the Cytoscape software (http://www.cytoscape.org)[33] to visualize the protein-protein interaction networks.

## Western Blotting

Western blotting was conducted as we described before[34]. Briefly, proteins treated with different concentrations of drugs were extracted from the cells and quantified. Equal amounts of protein were separated by electrophoresis on sodium dodecyl sulfate polyacrylamide gels and transferred to polyvinylidene fluoride membranes. The membranes were blocked with 5% non-fat milk in TBST (10 mM Tris-HCl, pH 7.4, 100 mM NaCl, 0.5% Tween-20) for 40 min at room temperature and incubated overnight at 4°C with primary antibodies (p-PDGFRα, Cell Signaling Technology, 3166, etc). The membranes were then washed in TBST and incubated with secondary antibodies (zsbio, ZB-2301) for 40 min. After extensive washing, membranes were visualized using the enhanced chemiluminescence reagent. Final images were analyzed using ImageJ.

## Immunofluorescence Staining Asssy

HUVECs administered with different concentrations of Lyc were grown at a 24-well plate after stimulated by PDGF-AA, fixed with 4% paraformaldehyde for 15 min and blocked with 5% bovine serum albumin for 1 h at room tempature. Sequently, primary antibody (p-PDGFRα, Thermofisher, 44-1000G) was applied to incubate the cells overnight and incubated with Alexa Fluor 488 secondary antibody (Thermofisher, A-11008) for 2 h. Finally, cells were incubated with hoechst (Thermofisher, 33258) for 5 min and visualized under an inverted fluorescent microscope.

## Molecular Docking

Molecular docking was performed using Schrödinger software, which included Protein Preparation Wizard, LigPrep, and Glide modules. PDGFRα crystal structure (PDB ID: 6JOK) was prepared from RCSB[35] and optimized with the Protein Preparation Wizard. LigPrep was used to generate multiple conformational states for Lyc ligand molecules. Docking between Lyc and PDGFRα with standard precision (SP) was performed by Glide[36, 37]. The rootmean-square deviation (RMSD) value was calculated from superimposed ligands to examine docking parameters that were capable of reproducing a similar conformation to that of the co-crystal at the active site of PDGFRα.

### PDGFRα Enzymatic Assay

PDGFRα enzymatic assay was performed using the Kinase Activity Assay Kit (Abace, Beijing, China) following the manufacturer's protocol. Purified human PDGFRα protein was treated with Lyc at different concentrations in a black 384-well plate. The fluorescence intensity was measured by an automatic microplate reader (Promega, USA).

### Biacore Assay for Surface Plasmon Resonance (SPR) Analysis

Surface plasmon resonance (SPR) affinity experiment[38, 39] for drug-target interaction analysis was conducted employing a Biacore 100 T biosensor detector (GE healthcenter, USA). Different concentrations of Lyc were injected to protein (Human PDGFRα Protein, His, Strep II Tag Protein [H5252]) and blank channels. The experiment was conducted at 25°C, the supernatant flow rate was 20 μl/min. 10 mM acetate was employed as immobilization buffer and 1 x PBS as running buffer.

### CElluar Thermal Shift Assays (CETSAs)

CETSAs were conducted to detect the direct binding between Lyc and PDGFRα in celluar. Briefly, cells were pre-treated with 6 uM of Lyc for 48 h, chilled on ice, washed with PBS containing protease inhibitor and then transferred into 1.5 ml PCR tubes and heated for 3 min at appropriate temperature. Subsequently, cells were lysed, seperated and detected by western blot assays.

### Statistical Methods

Results were analyzed using SPSS software (IL, USA). All experiments were independently repeated at least three times and data were presented as the mean ± SD. Student’ s two-tailed t-test and one-way ANOVA were performed to determine statistical significance between different groups. Differences were considered significant when p-values < 0.05.

## Results

### Lyc Inhibited Angiogenesis

Tumor blood vessels provide oxygen and nutrients necessary for the metabolism of tumor cells. Thus, angiogenesis is the most basic factor in the growth and metastasis of tumors. The proliferation and migration of vascular endothelial cells toward tumor cells via a gap in the basement membrane is a key step in tumor angiogenesis. The inhibitory effect of Lyc on the proliferation and migration of HUVECs was observed to explore its impact on angiogenesis. An MTT assay was used to determine the cell viability of HUVECs treated with Lyc at different concentrations and at different time points to detect the inhibitory effect of Lyc on the proliferation of HUVECs. As shown in Figure 1A, Lyc inhibited proliferation and promoted apoptosis of HUVECs in a concentration- and time-dependent manner ($IC_{50}$: 24 h 9.34 μM, 48 h 4.93 μM). To further evaluate the inhibitory effect of Lyc on the growth of HUVECs, we selected sunitinib, a commonly used anti-angiogenesis agent[40], as the standard reference drug. The results of the

MTT assay showed that 12 μM Lyc and 1 μM sunitinib (a commonly used concentration of sunitinib[41, 42]) had similar inhibitory effects (Figure 1B), while the combination of Lyc and sunitinib sharply decreased the viability of HUVECs, and the extent of reduced cell viability by the combination therapy was significantly greater than either of the monotherapies (Lyc or sunitinib). Further colony formation experiments were conducted to determine the inhibitory effect of Lyc on the proliferation of HUVECs. As shown in Figure 1C-D, Lyc and sunitinib both effectively decreased colony formation, and the combination treatment of Lyc and sunitinib decreased colony formation even more. Flow cytometry was used to determine whether Lyc caused changes in the apoptotic cell number (upper right quadrant: early apoptosis, lower right quadrant: late apoptosis). PI-annexin V staining showed that apoptotic cells increased after the addition of Lyc and/or sunitinib, with significant differences between the different treatments (Figure 1E). Next, we examined Lyc's antimigration effect on HUVECs. In the transwell assay, Lyc administration inhibited cell migration in a dose-dependent manner. The combination of Lyc and sunitinib resulted in fewer cells transferred to the lower transwell chamber (Figure 2A). Wound healing results also showed that the migration ability of HUVECs decreased with the use of Lyc and/or sunitinib (Figure 2B). HUVECs were treated with 0, 6 or 12 μM Lyc or 0 and 1 μM sunitinib, and Lyc was found to inhibit tube formation and significantly disrupt tube-like structure and vascular net formation (Figure 2C). The CAM assay is a unique ex vivo model used to investigate the process of angiogenesis and the effects of anti-angiogenic drugs. The effect of Lyc was thus evaluated using the CAM assay. Angiogenesis remained unchanged in the control group, while it was dramatically decreased by Lyc or sunitinib treatment, and neovascularization was further decreased after the combined use of Lyc and sunitinib (Figure 3). These results indicate that Lyc can inhibit angiogenesis.

## Identification of Lyc Targets using Bioinformatics

The structural formula for Lyc was uploaded to PharmMapper, and duplicate results were removed to obtain a total of 456 possible targets. The official symbols for the drug targets were obtained from UniProt. For a more in-depth understanding of the target protein, GO function and KEGG pathway analyses were applied in WebGestalt. Signal transduction was the most significant biological process (BP) term, cytoplasm and plasma membrane were the most significant cellular component (CC) terms, and protein binding was the most significant molecular function (MF) term (Figure 4A-C). The KEGG pathway analysis showed that the targets were involved in the MAPK/PI3K-AKT pathways (Figure 4D). A total of 4515 angiogenesis-related targets were obtained from the GeneCards database. The Lyc targets intersected with the angiogenesis-related targets. A total of 98 possible targets for Lyc inhibition of angiogenesis were obtained (Figure 4E). Among them, PDGFRα is the classical kinase that drives angiogenesis. Therefore, it was speculated that Lyc inhibited angiogenesis through PDGFRα (Figure 4F).

## Lyc Targeted PDGFRα

As mentioned above, PDGFRα was verified as Lyc's target using bioinformatics prediction. Ligand binding to PDGFRα causes dimerization of the receptors; this is a key event in activation since it brings the intracellular parts of the receptors close to each other, promoting autophosphorylation of the receptors.

The kinase is activated after autophosphorylation and binds to adaptor molecules, such as Grb2, to activate downstream MAPK/PI3K-AKT signaling pathways[43]. In this experiment, HUVECs were treated with different concentrations of Lyc, and western blotting was used to detect the changes in protein expression to clarify the regulatory effect of Lyc on PDGFRα pathways. Total PDGFRα expression did not change significantly after Lyc treatment, and the phosphorylation of PDGFRα (p-PDGFRα) was downregulated (Figure 5A). The phosphorylation levels and activation of downstream PI3K and AKT were also downregulated. Similar results were also observed in the immunofluorescence staining assay (Figure 5B). Elevated expression of p-PDGFRα was noted in the untreated HUVECs. Conversely, p-PDGFRα expression was remarkably decreased after trreatment with 6 or 12 μM Lyc. These results suggest that Lyc can inhibit the activation of PDGFRα.

## Lyc Docked to PDGFRα

Molecular docking predicts potential interactions of the proposed protein with a selected molecule, which is a structural modeling approach to study possible binding sites for cancer therapeutics. We applied molecular docking to explore the specific mechanism through with Lyc acts on its targets. Sunitinib was chosen as a positive control to investigate energy matching and geometrical complementarity. The results showed that Lyc and PDGFRα had good binding capacity, with a Glide score of -7.632 kcal/mol, which is similar to that of sunitinib (G-score: -7.748 kcal/mol). As shown in Figure 6A-B, both Lyc and sunitinib form hydrogen bonds with cysteine 677 (Cys 677) of PDGFRα. The length of the Lyc-PDGFRα complex was 4.14 Å, suggesting that Lyc and sunitinib may have similar effects on PDGFRα. For the ligand crystal (Lyc), benzo[d][1,3]dioxole extended deeper into the kinase active site, whereas (3S,31S,6aS,7S,8S)-7,8-dihydroxy-1,2,3,31,4,5,6,6a,7,8-decahydropyrrolo[3,2,1-ij]quinolin-3-ium extended toward the solvent. Next, the molecular docking was evaluated by redocking poses of the crystal structure and calculating RMSD. The docking method was considered accurate, while the calculated confirmation RMSD value was less than 2.0 Å[44]. The RMSD value of the poses obtained by docking methods was 0.9812 Å, and the docking could be considered accurate. In addition, Lyc and PDGFRα combined well without significant steric hindrance. Similar to the molecular docking results, the kinase activity assay showed that Lyc inhibited PDGFRα with an $IC_{50}$ of approximately 0.85 μM (Figure 6C). When we performed a Biacore experiment, the positive signals became more significant with increasing Lyc concentration. Lyc directly bound to PDGFRα in a concentration-dependent manner and had micromolar binding affinity ($K_D$ = 149.6 μM, Figure 6D-E). Finally, CETSAs were performed to determine the direct binding between PDGFRα protein and Lyc in cellulo. As shown in Figure 6F-G, Lyc administration obviously shifted the PDGFRα melting curve compared to the control. In summary, Lyc docks to PDGFRα to inhibit its activation.

## Lyc Inhibited PDGF-AA-induced Angiogenesis

As described above, PDGFRα is dimerized and activated by the ligand PDGF. The ligand/receptor interactions proven to be important in vivo are PDGF-AA and PDGF-CC, which induce PDGFRα dimerization. Therefore, we tested whether Lyc could inhibit PDGF-AA-induced angiogenesis. As shown in

Figure 7A, pretreatment of HUVECs with PDGF-AA (25 ng/ml) stimulated cell growth, which was restrained by Lyc administration. Lyc also prevented PDGF-AA-induced colony formation (Figure 7B). Similar to cell viability, Lyc also restrained PDGF-AA-induced HUVEC migration, and cell migration to the lower chamber was increased by PDGF-AA stimulation but decreased by Lyc administration (Figure 7C). In the tube formation assay, treatment of HUVECs with Lyc prevented HUVEC tube formation on the Matrigel matrix containing 25 ng/ml PDGF-AA (Figure 7D). When HUVECs were treated with Lyc (6 μM) and pretreated with PDGF-AA (25 ng/mL), it was evident that Lyc inhibited PDGF-AA-induced PDGFRα activation (Figure 7E). These results indicated that Lyc can inhibit angiogenesis by targeting PDGFRα.

# Discussion

Alkaloids are basic organic compounds containing nitrogen that mainly exist in plants and animals. Alkaloids have a complex ring structure, which mostly contains nitrogen. Based on this structure, alkaloids show rich physiological and pharmacological activities. Approximately 20 kinds of Lycoris SPP. are widely distributed in the world. Lycoris was the first alkaloid isolated from Lycoris spp., and it is also the most common alkaloid in this family[45]. In previous studies, Lyc was shown to inhibit the growth and metastasis of different tumor types, such as melanoma[46], colorectal cancer[47] and gastric cancer[48]. In our study, we found that Lyc inhibited angiogenesis. The ideal strategy of treating tumors relies on the use of one inhibitor targeting multiple tumor hallmarks rather than the use of several drugs that each target different tumor hallmarks. Studies have also shown that the combination of anti-proliferative and anti-angiogenic drugs can produce synergistic effects[49] . Therefore, we speculate that Lyc has a synergistic anti-proliferative and anti-angiogenic effect.

HUVECs extracted from the umbilical cord is an alternative model to study tumor angiogenesis. During proliferation and invasion, proteases secreted by tumor cells degrade the extracellular matrix (ECM), and immature vascular endothelial cells sprout into the tumor basement membrane. Then, vascular endothelial cells continue to mature and differentiate and form the vascular lumen. The capillary network further spreads and finally forms mature blood vessels[50]. The proliferation, migration and tubule formation of vascular endothelial cells are milestones in the middle and late stages of tumor angiogenesis[51]. Natural products represent a rich diversity of compounds and are currently being actively exploited to treat tumor angiogenesis[52]. In this study, through different assays, we found that Lyc inhibits the proliferation, migration and tube formation of HUVECs.

The CAM assay has the advantages of simple sampling, a short experimental period and simple operation. However, the disadvantages of the CAM assay are that the local damage caused by the change in osmotic pressure and pH value affect angiogenesis, and the experimental operation process and the state of the chicken embryo chorionic membrane also have a great influence on the experimental results[53-55]. In our study, after Lyc administration, angiogenesis on the chorioallantoic membrane decreased, indicating that Lyc can inhibit angiogenesis in the CAM assay.

The PDGFRA gene, which maps to chromosome 4q12, encodes a highly homologous transmembrane glycoprotein,named PDGFRα,that belongs to the type III receptor tyrosine kinase family.Binding of PDGF stimulates PDGFRα dimerization, which further initiates intracellular signaling[56]. In solid tumors, PDGFRα is expressed on nonmalignant cells, such as pericytes of vessels, and on fibroblasts and myofibroblasts of the stroma. The present study found that Lyc can inhibit the activation of PDGFRα by binding to it directly. D842V mutation in the PDGFRA 18 exon accounts for approximately 5% of cases, and these patients are resistant to traditional PDGFRα inhibitors[57, 58]. Using molecular docking, we found that Lyc not only docked to wild-type PDGFRα but also bound to mutant PDGFRα, but this observation needs to be confirmed by further experiments.

Cascade signaling pathway activation induced by PDGF/PDGFRα can regulate vascular endothelial cells, enhance vascular permeability, and regulate angiogenesis[59]. When the diameter of the tumor tissue reaches 1 cm, the tumor tissue synthesizes, secretes and releases PDGF through the para/autocrine mechanism. This enlarges the intercellular space of the capillary wall and exudates fibrinogen from the blood vessel wall to activate plasminogen and metalloproteinases in the matrix to form a tube network structure[60]. In our study, we found that Lyc inhibited PDGF-AA-induced angiogenesis.

Tyrosine kinase inhibitors (TKIs) bind to tyrosine residues in the intracellular region of membrane receptors and inhibit tyrosine phosphorylation, thereby preventing tumor-related signal activation. Molecular docking in computer-aided drug design (CADD) selects the optimal binding mode of the receptor and ligand according to the energy and spatial structure complementarity of the receptor and ligand. The reasonable relative position, molecular direction and dynamic change of receptor and ligand molecules are determined by molecular docking[61]. In this study, the benzo[d][1,3]dioxole in Lyc was speculated to dock to cysteine 677 in PDGFRα, which was further confirmed by different assays.

# Conclusion

Natural products have unique advantages in tumor treatment, but their effective substances and mechanisms are not yet clear; thus, the specific targets of natural products have not been identified. In this study, using bioinformatics prediction, molecular docking, and in vitro and ex vivo experiments, Lyc was shown to attenuate PDGFRα activation. In addition, natural products produce pharmacological effects on different targets, but this study only examined the role of Lyc on PDGFRα. The possible Lyc impact on other targets, especially other tyrosine kinases, needs to be further investigated. Clinical trials are the most critical step in the development of drugs and determining their applicability to extended indications. We look forward to clinical trials with large sample sizes to verify the efficacy of Lyc for the treatment of tumors.

# Declarations

### Ethics approval and consent to participate

Not applicable.

### Consent for publication

Not applicable

### Availability of data and materials

All data generated or analysed during this study are included in this published article and its supplementary information files.

### Competing interests

The author(s) declared no potential conflicts of interest with respect to the research, authorship, and/or publication of this article.


### Funding

The author(s) received no financial support for the research, authorship, and/or publication of this article.


### Authors' contributions

YW contributed to the conception and design of the study. FL and XL performed the experiments and statistical analyses. LH conducted computer science. FL prepared the first draft of the manuscript. All authors contributed to manuscript revision and have read and approved the submitted version.


### Acknowledgements

Not applicable.


### Authors' information


Fei Lv, Department of Oncology, Shengjing Hospital of China Medical University, Shenyang, Liaoning, China. E-mail: 627734249@qq.com.

XiaoQi Li, Department of Oncology, Shenyang Tenth People's Hospital, Shenyang, Liaoning, China. E-mail: sddjw2016@126.com.

LiYing Hao, Department of drug toxicology, China Medical University, Shenyang, Liaoning, China. E-mail: 20201136@cmu.edu.cn.

Ying Wang, Department of Oncology, Shengjing Hospital of China Medical University, Shenyang, Liaoning, China. E-mail: wang_ying@sj.hospital.org.


## References

1. Sung H, Ferlay J, Siegel R L, et al. Global Cancer Statistics 2020: GLOBOCAN Estimates of Incidence and Mortality Worldwide for 36 Cancers in 185 Countries. CA Cancer J Clin, 2021,71(3):209-249.
2. Hanahan D, Weinberg R A. The hallmarks of cancer. Cell, 2000,100(1):57-70.
3. Melegh Z, Oltean S. Targeting Angiogenesis in Prostate Cancer. Int J Mol Sci, 2019,20(11).
4. Zhang Z, Ji S, Zhang B, et al. Role of angiogenesis in pancreatic cancer biology and therapy. Biomed Pharmacother, 2018,108:1135-1140.
5. Lugano R, Ramachandran M, Dimberg A. Tumor angiogenesis: causes, consequences, challenges and opportunities. Cell Mol Life Sci, 2020,77(9):1745-1770.
6. Finn R S, Qin S, Ikeda M, et al. Atezolizumab plus Bevacizumab in Unresectable Hepatocellular Carcinoma. N Engl J Med, 2020,382(20):1894-1905.
7. Liu X, Qin S, Wang Z, et al. Early presence of anti-angiogenesis-related adverse events as a potential biomarker of antitumor efficacy in metastatic gastric cancer patients treated with apatinib: a cohort study. J Hematol Oncol, 2017,10(1):153.
8. Liang X J, Shen J. Adverse events risk associated with angiogenesis inhibitors addition to therapy in ovarian cancer: a meta-analysis of randomized controlled trials. Eur Rev Med Pharmacol Sci, 2016,20(12):2701-2709.
9. Kim A, Ha J, Kim J, et al. Natural Products for Pancreatic Cancer Treatment: From Traditional Medicine to Modern Drug Discovery. Nutrients, 2021,13(11).
10. Yang Y, Liu Q, Shi X, et al. Advances in plant-derived natural products for antitumor immunotherapy. Arch Pharm Res, 2021,44(11):987-1011.
11. Li R, Song X, Guo Y, et al. Natural Products: A Promising Therapeutics for Targeting Tumor Angiogenesis. Front Oncol, 2021,11:772915.
12. Kaya G I, Cicek D, Sarikaya B, et al. HPLC - DAD analysis of lycorine in Amaryllidaceae species. Nat Prod Commun, 2010,5(6):873-876.
13. Wu J, Fu Y, Wu Y X, et al. Lycorine ameliorates isoproterenol-induced cardiac dysfunction mainly via inhibiting inflammation, fibrosis, oxidative stress and apoptosis. Bioengineered, 2021,12(1):5583-5594.
14. Lv X, Zhang M, Yu S, et al. Antiviral and virucidal activities of lycorine on duck tembusu virus in vitro by blocking viral internalization and entry. Poult Sci, 2021,100(10):101404.
15. Shen J W, Ruan Y, Ren W, et al. Lycorine: a potential broad-spectrum agent against crop pathogenic fungi. J Microbiol Biotechnol, 2014,24(3):354-358.
16. Roy M, Liang L, Xiao X, et al. Lycorine: A prospective natural lead for anticancer drug discovery. Biomed Pharmacother, 2018,107:615-624.
17. Shawky E, Takla S S, Hammoda H M, et al. Evaluation of the influence of green extraction solvents on the cytotoxic activities of Crinum (Amaryllidaeae) alkaloid extracts using in-vitro-in-silico approach. J Ethnopharmacol, 2018,227:139-149.

18. Shen J, Zhang T, Cheng Z, et al. Lycorine inhibits glioblastoma multiforme growth through EGFR suppression. J Exp Clin Cancer Res, 2018,37(1):157.
19. Yin S, Yang S, Luo Y, et al. Cyclin-dependent kinase 1 as a potential target for lycorine against hepatocellular carcinoma. Biochem Pharmacol, 2021,193:114806.
20. Zhao Z, Xiang S, Qi J, et al. Correction of the tumor suppressor Salvador homolog-1 deficiency in tumors by lycorine as a new strategy in lung cancer therapy. Cell Death Dis, 2020,11(5):387.
21. Yuan X H, Zhang P, Yu T T, et al. Lycorine inhibits tumor growth of human osteosarcoma cells by blocking Wnt/beta-catenin, ERK1/2/MAPK and PI3K/AKT signaling pathway. Am J Transl Res, 2020,12(9):5381-5398.
22. Ning L, Wan S, Jie Z, et al. Lycorine Induces Apoptosis and G1 Phase Arrest Through ROS/p38 MAPK Signaling Pathway in Human Osteosarcoma Cells In Vitro and In Vivo. Spine (Phila Pa 1976), 2020,45(3):E126-E139.
23. Yu H, Qiu Y, Pang X, et al. Lycorine Promotes Autophagy and Apoptosis via TCRP1/Akt/mTOR Axis Inactivation in Human Hepatocellular Carcinoma. Mol Cancer Ther, 2017,16(12):2711-2723.
24. Liu R, Cao Z, Tu J, et al. Lycorine hydrochloride inhibits metastatic melanoma cell-dominant vasculogenic mimicry. Pigment Cell Melanoma Res, 2012,25(5):630-638.
25. Cao Z, Yu D, Fu S, et al. Lycorine hydrochloride selectively inhibits human ovarian cancer cell proliferation and tumor neovascularization with very low toxicity. Toxicol Lett, 2013,218(2):174-185.
26. Giacomelli L, Covani U. Bioinformatics and data mining studies in oral genomics and proteomics: new trends and challenges. Open Dent J, 2010,4:67-71.
27. Gao L, Feng Y, Ge C, et al. Identification of molecular anti-metastasis mechanisms of lycorine in colorectal cancer by RNA-seq analysis. Phytomedicine, 2021,85:153530.
28. Liu X, Ouyang S, Yu B, et al. PharmMapper server: a web server for potential drug target identification using pharmacophore mapping approach. Nucleic Acids Res, 2010,38(Web Server issue):W609-W614.
29. Ashburner M, Ball C A, Blake J A, et al. Gene ontology: tool for the unification of biology. The Gene Ontology Consortium. Nat Genet, 2000,25(1):25-29.
30. Kanehisa M, Goto S. KEGG: kyoto encyclopedia of genes and genomes. Nucleic Acids Res, 2000,28(1):27-30.
31. Ogata H, Goto S, Sato K, et al. KEGG: Kyoto Encyclopedia of Genes and Genomes. Nucleic Acids Res, 1999,27(1):29-34.
32. Zhang B, Kirov S, Snoddy J. WebGestalt: an integrated system for exploring gene sets in various biological contexts. Nucleic Acids Res, 2005,33(Web Server issue):W741-W748.
33. Saito R, Smoot M E, Ono K, et al. A travel guide to Cytoscape plugins. Nat Methods, 2012,9(11):1069-1076.
34. Lv F, Deng M, Bai J, et al. Piperlongumine inhibits head and neck squamous cell carcinoma proliferation by docking to Akt. Phytother Res, 2020,34(12):3345-3358.

35. Rose P W, Prlic A, Altunkaya A, et al. The RCSB protein data bank: integrative view of protein, gene and 3D structural information. Nucleic Acids Res, 2017,45(D1):D271-D281.
36. Friesner R A, Banks J L, Murphy R B, et al. Glide: a new approach for rapid, accurate docking and scoring. 1. Method and assessment of docking accuracy. J Med Chem, 2004,47(7):1739-1749.
37. Halgren T A, Murphy R B, Friesner R A, et al. Glide: a new approach for rapid, accurate docking and scoring. 2. Enrichment factors in database screening. J Med Chem, 2004,47(7):1750-1759.
38. Leonard P, Hearty S, Ma H, et al. Measuring Protein-Protein Interactions Using Biacore. Methods Mol Biol, 2017,1485:339-354.
39. Leonard P, Hearty S, O'Kennedy R. Measuring protein-protein interactions using Biacore. Methods Mol Biol, 2011,681:403-418.
40. de Bouard S, Herlin P, Christensen J G, et al. Antiangiogenic and anti-invasive effects of sunitinib on experimental human glioblastoma. Neuro Oncol, 2007,9(4):412-423.
41. Gu J, Zhang Y, Han Z, et al. Targeting the ERbeta/Angiopoietin-2/Tie-2 signaling-mediated angiogenesis with the FDA-approved anti-estrogen Faslodex to increase the Sunitinib sensitivity in RCC. Cell Death Dis, 2020,11(5):367.
42. Zhang H P, Takayama K, Su B, et al. Effect of sunitinib combined with ionizing radiation on endothelial cells. J Radiat Res, 2011,52(1):1-8.
43. Zhang P, Li S, Chen Z, et al. LncRNA SNHG8 promotes proliferation and invasion of gastric cancer cells by targeting the miR-491/PDGFRA axis. Hum Cell, 2020,33(1):123-130.
44. Nguyen C T, Tanaka K, Cao Y, et al. Computational Analysis of the Ligand Binding Site of the Extracellular ATP Receptor, DORN1. PLoS One, 2016,11(9):e161894.
45. Roy M, Liang L, Xiao X, et al. Lycorine: A prospective natural lead for anticancer drug discovery. Biomed Pharmacother, 2018,107:615-624.
46. Shi S, Li C, Zhang Y, et al. Lycorine hydrochloride inhibits melanoma cell proliferation, migration and invasion via down-regulating p21(Cip1/WAF1). Am J Cancer Res, 2021,11(4):1391-1409.
47. Gao L, Feng Y, Ge C, et al. Identification of molecular anti-metastasis mechanisms of lycorine in colorectal cancer by RNA-seq analysis. Phytomedicine, 2021,85:153530.
48. Li C, Deng C, Pan G, et al. Lycorine hydrochloride inhibits cell proliferation and induces apoptosis through promoting FBXW7-MCL1 axis in gastric cancer. J Exp Clin Cancer Res, 2020,39(1):230.
49. Huang C Y, Yu L C. Pathophysiological mechanisms of death resistance in colorectal carcinoma. World J Gastroenterol, 2015,21(41):11777-11792.
50. Mongiat M, Buraschi S, Andreuzzi E, et al. Extracellular matrix: the gatekeeper of tumor angiogenesis. Biochem Soc Trans, 2019,47(5):1543-1555.
51. Carmeliet P, Jain R K. Molecular mechanisms and clinical applications of angiogenesis. Nature, 2011,473(7347):298-307.
52. Shanmugam M K, Warrier S, Kumar A P, et al. Potential Role of Natural Compounds as Anti-Angiogenic Agents in Cancer. Curr Vasc Pharmacol, 2017,15(6):503-519.

53. Ribatti D. The chick embryo chorioallantoic membrane as a model for tumor biology. Exp Cell Res, 2014,328(2):314-324.
54. Ribatti D, Tamma R. The chick embryo chorioallantoic membrane as an in vivo experimental model to study multiple myeloma. Enzymes, 2019,46:23-35.
55. Pluchino N, Poppi G, Yart L, et al. Effect of local aromatase inhibition in endometriosis using a new chick embryo chorioallantoic membrane model. J Cell Mol Med, 2019,23(8):5808-5812.
56. Sil S, Periyasamy P, Thangaraj A, et al. PDGF/PDGFR axis in the neural systems. Mol Aspects Med, 2018,62:63-74.
57. Al-Share B, Alloghbi A, Al H M, et al. Gastrointestinal stromal tumor: a review of current and emerging therapies. Cancer Metastasis Rev, 2021,40(2):625-641.
58. Liang L, Yan X E, Yin Y, et al. Structural and biochemical studies of the PDGFRA kinase domain. Biochem Biophys Res Commun, 2016,477(4):667-672.
59. Franchini A, Malagoli D, Ottaviani E. Cytokines and invertebrates: TGF-beta and PDGF. Curr Pharm Des, 2006,12(24):3025-3031.
60. Gianni-Barrera R, Bartolomeo M, Vollmar B, et al. Split for the cure: VEGF, PDGF-BB and intussusception in therapeutic angiogenesis. Biochem Soc Trans, 2014,42(6):1637-1642.
61. Dong D, Xu Z, Zhong W, et al. Parallelization of Molecular Docking: A Review. Curr Top Med Chem, 2018,18(12):1015-1028.

# Figures

### Figure 1

Lyc inhibited HUVECs proliferation in vitro. (A) Time- and concentration- dependent inhibitory effect of Lyc on HUVECs. HUVECs were treated with Lyc and the cell viability was analyzed by MTT assay. The raw data of Figure 1A contained in Supplementary Information 1. (B) The synergetic effect of Lyc and sunitinib in 24 h was also measured by MTT assay. The raw data of Figure 1B contained in Supplementary Information 2. (C, D) Lyc and/or sunitinib inhibited colony formation significantly on HUVECs. Cells were treated with different concentrations of drugs and the colony formation was analyzed and shown in bar graphs (D). (E) Flow cytometry analysis. Cells were treated with different concentrations of drugs for 24 h and apoptotic intensity was analyzed by flow cytometry. Data represents mean ± SD, *$p < 0.05$, $n = 3$.

### Figure 2

Lyc inhibited HUVECs migration and tube formation in vitro. (A) Transwell assay was performed to measure cell migration in HUVECs treated with Lyc and/or sunitinib. The relative migration of cells was quantified. (B) Wound healing assay was used to detect migration distances of these cells treated with Lyc and/or sunitinib for different time. The quantification of relative wound area was performed. (C) Tube formation assay detected formed tubes of HUVECs treated with Lyc and/or sunitinib. Calculating branch points per field was used to quantify the ability of tube formation. The bar graphs represented quantification were shown in the bottom. Data represents mean ± SD, *p < 0.05, n = 3.

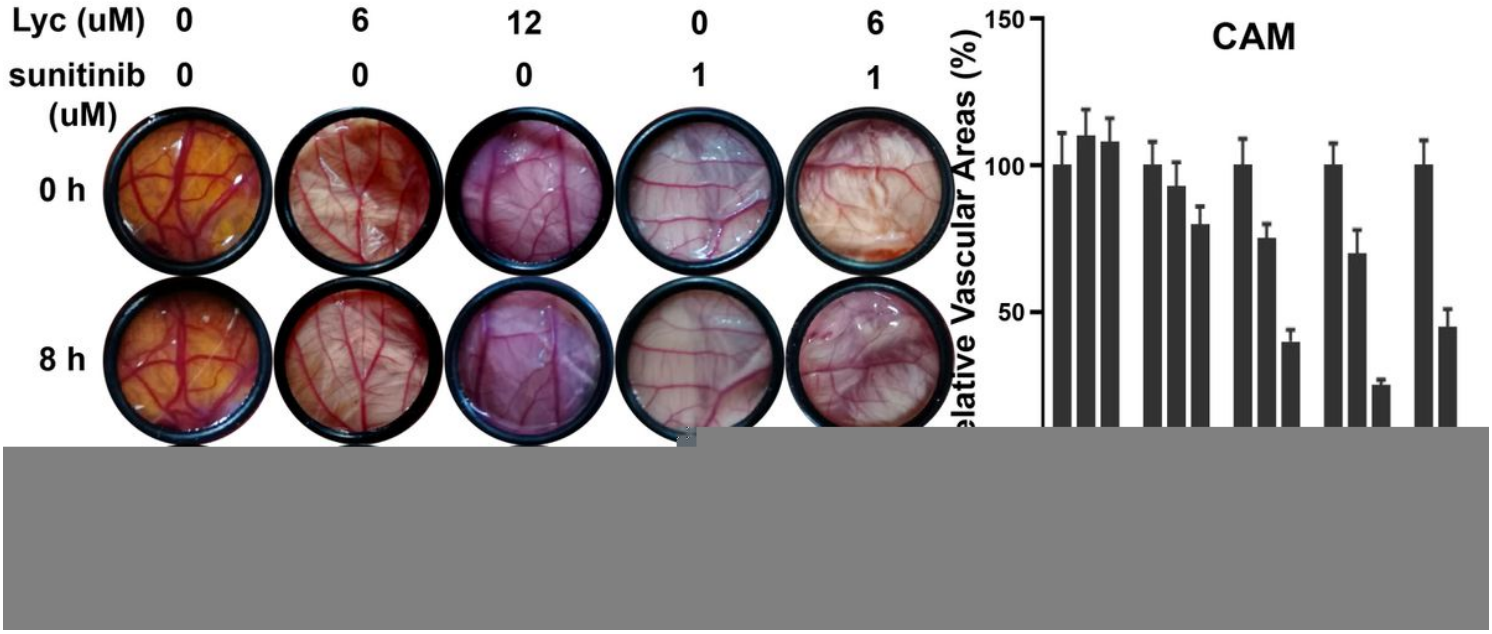


## Figure 3

CAM models were used to evaluate the anti-angiogenesis effect of Lyc and/or sunitinib ex vivo. Vascular area in each group was measured and compared by image-pro-plus 6.0. Bar graphs represent the relative vascular area. Data represents mean ± SD, *p < 0.05, n = 3.

## Figure 4

Bioinformatics prediction of Lyc targets. (A-C) Top 20 enriched Gene Ontology (GO) term enrichment analysis of Lyc targets, with the domains of biological processes (BP, A), cellular components (CC, B), and molecular functions (MF, C). The length of bars presented the gene counts and the gradation of color stood for the value of the minus log10 adjusted P value. (D) KEGG pathway enrichment analysis of Lyc targets with the top 20 enrichment scores. The size of the dot depicted the gene counts; the gradation of color stood for the value of minus log10 P value. (E) Identification of Lyc's targets on angiogenesis in Pharmmapper and Genecards. A total of 98 common targets for drugs and diseases are obtained. (F) Network of Lyc targets protein-protein interaction (PPI). The raw data of Figure 4 contained in Supplementary Information.

**Figure 5**

Lyc inhibited PDGFRα activition and virtual verification of Lyc targets by molecular docking. (A) Western blot analysis of total-cell extracts of HUVECs treated with Lyc for 24 h to evaluate the effect of Lyc on PDGFRα. Proteins in PDGFRα pathways, including PDGFRα, PI3K and AKT, were measured by western blotting. β-actin was used as internal control. The raw data of Figure 5A contained in Supplementary File 4. (B) P-PDGFRα expression was assessed by immunofluorescence staining. Nuclei were visualized with hoechst (blue). Scale bars represented 100 um. The bar graphes in the lower right corner represented relative expression level of p-PDGFRα in western blotting and immunofluorescence staining.

**Figure 6**

Lyc attenuated PDGFRα activition by binding to it directly. (A, B) Maestro 2D interactions between PDGFRα and sunitinib (A) or Lyc (B). Residues in green spheres are hydrophobic, blue spheres are polar, red spheres are negatively charged, purple spheres are charged and light yellow spheres are glycine. The purple arrows and their directions represent hydrogen bonds between the ligand and the protein. The green line represents the π-π stacking arrangement seen between the aromatic core. (C) Kinase activity assays were conducted to validate the inhibition of Lyc on PDGFRα kinase activity. Staurosporine, an effective protein kinase inhibitor, was chosen as positive control. (D) Biacore analysis results of Lyc and PDGFRα. The black dot represented various concentrations of Lyc, Lyc bound to PDGFRα with a KD of 149.6 uM. (F) Sensorgram of the interaction between Lyc and PDGFRα. (F, G) We conducted CETSAs and PDGFRα protein expression was detected by western blotting (F). The line chart showed the relative expression level of PDGFRα (G). The raw data of Figure 6 contained in Supplementary File 5.

**Figure 7**

Lyc inhibited PDGF-AA induced angiogenesis. (A) Lyc inhibited PDGF-AA induced HUVECs growth. The raw data of Figure 7A contained in Supplementary File 6. (B) Lyc inhibited PDGF-AA induced colony formation of HUVECs. (C) Lyc inhibited migration of EGF-treated HUVECs. (D) PDGF-AA increased tube formation in HUVECs, while Lyc destroyed tubular structure. (E) HUVECs were treated with Lyc after stimulated with PDGF-AA, then the western blot was applied to measure protein levels. The raw data of Figure 7E contained in Supplementary File 7.

# Supplementary Files

This is a list of supplementary files associated with this preprint. Click to download.

- SupplementaryInformation1.xlsx
- SupplementaryInformation2.xlsx
- SupplementaryInformation3.xlsx
- SupplementaryInformation4.xlsx
- SupplementaryInformation5.xlsx
- SupplementaryInformation6.xlsx
- SupplementaryInformation7.xlsx